International Symposium: "Advances in Nuclear Many-Body Theory",
Primosten, Croatia, June 7-10, 2011
Dedicated to Prof. Peter Ring on the occasion of his 70th birthday

Effects of triaxiality in low-lying states of magnesium isotopes: a relativistic 3DAMP+GCM study

Jiangming Yao (尧江明)

Physique Nucléaire Théorique et Physique Mathématique,
Université Libre de Bruxelles, C.P. 229, B-1050 Bruxelles, Belgium

School of Physical Science and Technology,
Southwest University, Chongqing, 400715 China

June 9, 2011

ULB UNIVERSITÉ LIBRE DE BRUXELLES, UNIVERSITÉ D'EUROPE

Outline

1. **Introduction**
   - Importance of triaxial deformation
   - Beyond mean-field study of nuclear low-lying states
2. **The relativistic 3DAMP+GCM model**
   - Introduction to the model
   - Approximate correction scheme for particle number
3. **Low-lying states of magnesium isotopes**
   - Shape evolution and triaxiality
   - Triaxiality and pairing correlations in ^{30,32}Mg
4. **Summary and perspective**

Importance of triaxial deformation in atomic nuclei

Triaxiality has already been found to be very important in

1. bulk properties of nuclear ground state:
   - In the FRLDM calculations *[Moller2006]*: the systematic deviation between calculated and measured masses could be removed after including the triaxiality.

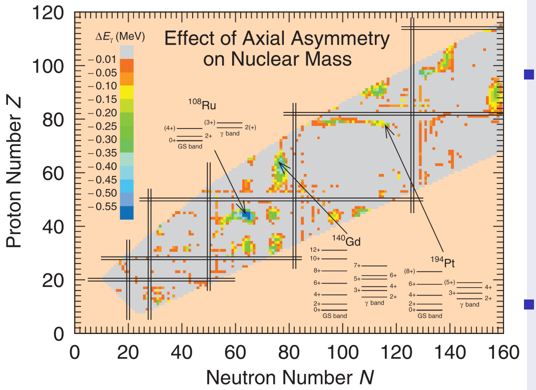

- The lowering of nuclear ground-state energy when axial symmetry is broken, relative to calculations limited to axially symmetric shapes only. Taken from the FRLDM calculations in Ref. *P. Moller et al., PRL 97, 162502 (2006)*.
- Several islands of triaxiality are observed.

Importance of triaxial deformation in atomic nuclei

Triaxiality has already been found to be very important in

1. bulk properties of nuclear ground state:
   - In the FRLDM calculations *[Moller2006]*: the systematic deviation between calculated and measured masses could be removed after including the triaxiality.
   - In the HFB+Gogny force calculations *[Rodriguez-Guzman2010]*: Compared with the steep behavior for neighboring Sr and Zr isotopes, the smooth changing in the isotopic dependence of the charge radii for Mo isotopes.
2. nuclear cluster decay, fission barrier (^{240}Pu), $\cdots$

Importance of triaxial deformation in atomic nuclei

Triaxiality has already been found to be very important in

1. bulk properties of nuclear ground state:
   - In the FRLDM calculations *[Moller2006]*: the systematic deviation between calculated and measured masses could be removed after including the triaxiality.
   - In the HFB+Gogny force calculations *[Rodriguez-Guzman2010]*: Compared with the steep behavior for neighboring Sr and Zr isotopes, the smooth changing in the isotopic dependence of the charge radii for Mo isotopes.
2. nuclear cluster decay, fission barrier (^{240}Pu), $\cdots$
3. high-spin nuclear structure
   - chiral rotations *[Frauendorf1997,Grodner2006]* and wobbling motion *[Odegard2001]*.
   - violation of the K-selection rule in electromagnetic transitions of high-spin isomers *[Chowdhury1988]*.

Importance of triaxial deformation in atomic nuclei

Triaxiality has already been found to be very important in

1. bulk properties of nuclear ground state:
   - In the FRLDM calculations *[Moller2006]*: the systematic deviation between calculated and measured masses could be removed after including the triaxiality.
   - In the HFB+Gogny force calculations *[Rodriguez-Guzman2010]*: Compared with the steep behavior for neighboring Sr and Zr isotopes, the smooth changing in the isotopic dependence of the charge radii for Mo isotopes.
2. nuclear cluster decay, fission barrier (^{240}Pu), $\cdots$
3. high-spin nuclear structure
   - chiral rotations *[Frauendorf1997,Grodner2006]* and wobbling motion *[Odegard2001]*.
   - violation of the K-selection rule in electromagnetic transitions of high-spin isomers *[Chowdhury1988]*.
4. **low-spin nuclear structure**
   - **height of barrier separating prolate and oblate minima: shape-coexistence (^{74,76}Kr) *[Clément2007]* or just γ-soft or the oblate saddle point?**
   - **electromagnetic transition strengthes: $E0, E2$ and $M1$, g-factor, $\cdots$**
   - **excitation spectra of g.s. band and γ-band?**

Beyond the self-consistent mean-field theory: Recent progress

In the past decade, several beyond self-consistent mean-field (Multi-Reference EDF) models have been developed that perform the restoration of symmetries broken by the static nuclear mean field, and take into account fluctuations around the mean-field minimum. These models have been applied to study nuclear low-spin states.

Restricted to axial shape

- PNP+1DAMP+GCM (HF with Skyrme force)
  A. Valor, P.-H. Heenen, and P. Bonche, NPA671, 145(2000)
- PNP+1DAMP+GCM (HFB with Gogny force)
  R. Rodriguez-Guzman, J. L. Egido, and L. M. Robledo, NPA709, 201(2002)
- PNP+1DAMP+GCM (RMF with point-coupling force)
  T. Niksic, D. Vretenar, and P. Ring, PRC73, 034308 (2006)

Beyond the self-consistent mean-field theory: Recent progress

In the past decade, several beyond self-consistent mean-field (Multi-Reference EDF) models have been developed that perform the restoration of symmetries broken by the static nuclear mean field, and take into account fluctuations around the mean-field minimum. These models have been applied to study nuclear low-spin states.

Restricted to axial shape

- PNP+1DAMP+GCM (HF with Skyrme force)
  A. Valor, P.-H. Heenen, and P. Bonche, NPA671, 145(2000)
- PNP+1DAMP+GCM (HFB with Gogny force)
  R. Rodriguez-Guzman, J. L. Egido, and L. M. Robledo, NPA709, 201(2002)
- PNP+1DAMP+GCM (RMF with point-coupling force)
  T. Niksic, D. Vretenar, and P. Ring, PRC73, 034308 (2006)

Applications for nuclear low-lying states

- low-spin normal-deformed and super-deformed collective states
  Bender, Flocard & Heenen, PRC68, 044321 (2003)
- shape coexistence in Kr, Pb isotopes
  Rodriguez-Guzman, Egido & Robledo, PRC 69, 054319 (2004);
  Bender, Bonche & Heenen, PRC 74, 024312 (2006)
- shell closures at N=32 or 34?
  Rodriguez & Egido, PRL 99, 062501 (2007)
- shape transition in Nd isotopes
  Niksic, Vretenar, Lalazissis & Ring, PRL99, 092502 (2007);

Beyond the self-consistent mean-field theory: Recent progress

What's the influence of triaxiality in the studies of above phenomena (shape coexistence, shape phase transition, shell closure, etc.)?

Beyond the self-consistent mean-field theory: Recent progress

What's the influence of triaxiality in the studies of above phenomena (shape coexistence, shape phase transition, shell closure, etc.)?

To answer this question, several collective models with allowing for the triaxial deformation have been developed based on the SC mean-field (EDF) calculations to study the nuclear low-lying states.

EDF based Bohr-Hamiltonian

- HFB with Gogny force
  J. Libert, M. Girod, and J.-P. Delaroche, PRC60, 054301 (1999)
- HF+BCS with Skyrme force
  L. Prochniak, P. Quentin, D. Samsoen, and J. Libert, NPA730, 59 (2004)
- RMF+BCS/RHB with point-coupling force
  T. Niksic, Z. P. Li, D. Vretenar, L. Prochniak, J. Meng and P. Ring, PRC79, 034303 (2009)

EDF mapped hybrid collective models

- *K. Nomura et al., PRL101, 142501 (2008)*
- *N. Hinohara et al., PRC82, 064313 (2010)*
- . . .

Beyond the self-consistent mean-field theory: Recent progress

What's the influence of triaxiality in the studies of above phenomena (shape coexistence, shape phase transition, shell closure, etc.)?

To answer this question, several collective models with allowing for the triaxial deformation have been developed based on the SC mean-field (EDF) calculations to study the nuclear low-lying states.

EDF based Bohr-Hamiltonian

- HFB with Gogny force
  J. Libert, M. Girod, and J.-P. Delaroche, PRC60, 054301 (1999)
- HF+BCS with Skyrme force
  L. Prochniak, P. Quentin, D. Samsoen, and J. Libert, NPA730, 59 (2004)
- RMF+BCS/RHB with point-coupling force
  T. Niksic, Z. P. Li, D. Vretenar, L. Prochniak, J. Meng and P. Ring, PRC79, 034303 (2009)

EDF mapped hybrid collective models

- *K. Nomura et al., PRL101, 142501 (2008)*
- *N. Hinohara et al., PRC82, 064313 (2010)*
- ...

In comparison with MR-EDF

In these collective models, the contribution from the off-diagonal elements $\langle\Phi(q)|\hat{O}|\Phi(q')\rangle$, with $q \neq q'$, is not, or only partially considered. The validity of this approximation is unknown.

Beyond the self-consistent mean-field theory: Recent progress

In recent years, the MR-EDF framework has been extended to allow for triaxial deformation, which makes it possible to study the nuclear low-lying states with the consideration of effects from

1. restoration of rotation symmetry in full 3D Euler space
2. shape fluctuation in full β-γ plane

Non-relativistic MR-EDF

- PNP+3DAMP+GCM (HFB with Skyrme force)
  M. Bender and P.-H. Heenen, PRC78, 024309 (2008).
- PNP+3DAMP+GCM (HFB with Gogny force)
  T. R. Rodriguez and J. L. Egido, Phys. Rev. C 81, 064323 (2010)

Only illustrative calculations have been carried out in non-relativistic frameworks because of extremely time-consuming !

Beyond the self-consistent mean-field theory: Recent progress

In recent years, the MR-EDF framework has been extended to allow for triaxial deformation, which makes it possible to study the nuclear low-lying states with the consideration of effects from

1. restoration of rotation symmetry in full 3D Euler space
2. shape fluctuation in full β-γ plane

Non-relativistic MR-EDF

- PNP+3DAMP+GCM (HFB with Skyrme force)
  M. Bender and P.-H. Heenen, PRC78, 024309 (2008).
- PNP+3DAMP+GCM (HFB with Gogny force)
  T. R. Rodriguez and J. L. Egido, Phys. Rev. C 81, 064323 (2010)

Only illustrative calculations have been carried out in non-relativistic frameworks because of extremely time-consuming !

In this talk, I am going to introduce

1. framework of our relativistic 3DAMP+GCM model
2. application to the nuclear low-lying states of magnesium isotopes
3. the effects of triaxiality and pairing correlation

Outline

The relativistic 3DAMP+GCM model

Intrinsic states from the relativistic mean-field calculations

1. The relativistic point-coupling model+BCS calculations with constraints on quadrupole moments by minimizing the energy functional

$$E'[\rho_i, j_i^\mu, \kappa] = E[\rho_i, j_i^\mu, \kappa] + \sum_{\mu=0,2} \frac{C_\mu}{2}(\langle \hat{Q}_{2\mu}\rangle - q_{2\mu})^2 \tag{1}$$

generate a large set of highly correlated triaxially deformed states $|\Phi(q)\rangle$.

- To study the nuclear-lying state with proper symmetries, this SR-EDF is extended to MR-EDF with the projection technique.
- The parameters in the EDF have been determined by fitting to the properties of nuclear matter and ground state of finite nuclei.
  PC-F1: Burvenich, Madland, Maruhn & Reinhard, PRC65, 044308 (2002).
  DD-PC1: Niksic, Vretenar & Ring, PRC78, 034318 (2008).
  PC-PK1: Zhao, Li, Yao & Meng, PRC82, 054319 (2010).

The relativistic 3DAMP+GCM model

Configuration mixing of angular momentum projected triaxial states

2. The nuclear wavefunction of even-even nucleus with good angular momentum J and shape fluctuation in deformations (β, γ) is obtained by projecting the intrinsic states $|\Phi(\beta,\gamma)\rangle$ onto good angular momentum (K-mixing) and performing GCM calculations (configuration mixing),

$$|\Psi_\alpha^{JM}\rangle = \int d\beta d\gamma \sum_{K\geq 0} f_\alpha^{JK}(\beta,\gamma) \underbrace{\frac{1}{(1+\delta_{K0})}[\hat{P}^J_{MK} + (-1)^J \hat{P}^J_{M-K}]}|\Phi(\beta,\gamma)\rangle, \quad (2)$$

where $|\Phi(\beta,\gamma)\rangle$ is a set of quasi-particle vacua from the constrained RMF+BCS calculations. The coefficients f_α^{JK} and excitation energies E_α^J are determined from the solution of Hill-Wheeler-Griffin (HWG) integral equation: $q \equiv (\beta,\gamma)$

$$\int dq' \sum_{K'\geq 0} \left[\mathscr{H}^J_{KK'}(q,q') - E^J_\alpha \mathscr{N}^J_{KK'}(q,q')\right] f_\alpha^{JK'}(q') = 0, \quad (3)$$

where $\mathscr{H}$ and $\mathscr{N}$ are the angular-momentum projected GCM kernel matrices of the Hamiltonian and the Norm, respectively.

The relativistic 3DAMP+GCM model

Evaluation of observable

3. The electromagnetic moments and transition strengths are evaluated with the nuclear wavefunctions.

- $E0$ and $E2$ transition strengths

$$B(\sigma\lambda; J_i, \alpha_i \to J_f, \alpha_f) = \frac{e^2}{2J_i+1} \sum_{M_i \mu M_f} \left| \langle J_f, M_f, \alpha_f | \hat{M}(\sigma\lambda\mu) | J_i, M_i, \alpha_i \rangle \right|^2 \quad (4)$$

- g-factor: $\mu(J^\pi)/J$
- Spectroscopic quadrupole moment: $Q^{\rm spec}(J)$

Note: Since all the matrix elements are calculated in the full configuration space, there is no need for effective charges.

particle number correction

Approximate correction scheme for particle number

Subtracting two constraining terms [Hara82,Bonche90],

$$-\lambda_p[Z(\mathbf{r};q,q';\Omega)-Z_0]-\lambda_n[N(\mathbf{r};q,q';\Omega)-N_0], \qquad (5)$$

from the transition energy functional. $Z_0(N_0)$ is the desired proton (neutron) number. $Z(\mathbf{r};q,q';\Omega)$ or $N(\mathbf{r};q,q';\Omega)$ is the corresponding transition density.

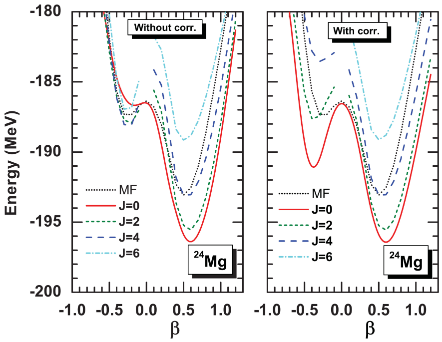

- Mean-field and angular-momentum projected potential energy curves of ^{24}Mg, calculated without (left panel) and with (right panel) the particle-number correction.
- Importance of the particle-number correction on the ordering of angular-momentum projected PECs in certain regions of deformation.

Outline

Potential energy curves

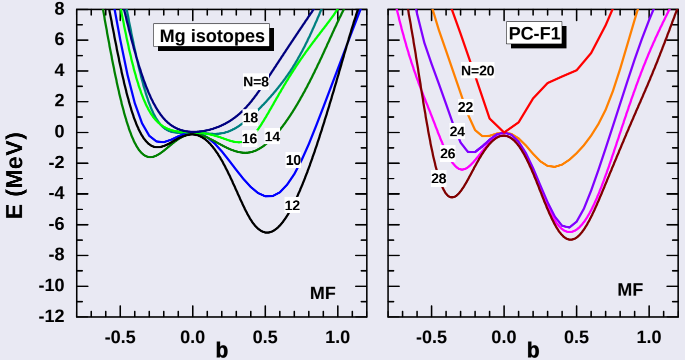

Figure: Self-consistent RMF+BCS mean-field potential energy curves of even-even magnesium isotopes, as functions of the axial deformation parameter β.

There are both prolate and oblate minima in most isotopes. The changing of global minima shows a clear picture of shape evolution with the neutron number: spherical (N=8) $\longrightarrow$ deformed $\longrightarrow$ spherical (N=20) $\longrightarrow$ deformed

Potential energy curves

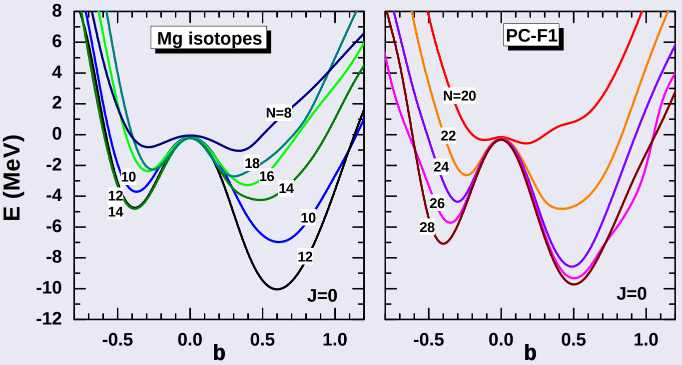

Figure: Angular-momentum projected 0^+ potential energy curves of even-even magnesium isotopes, as functions of the axial deformation parameter β.

The restoration of rotational symmetry lowers down the deformed minima and makes the spherical minima soft.

Nuclear shape and shell structure

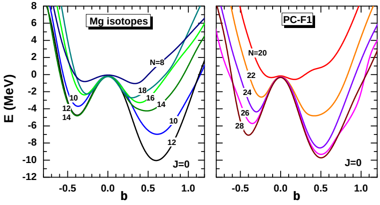

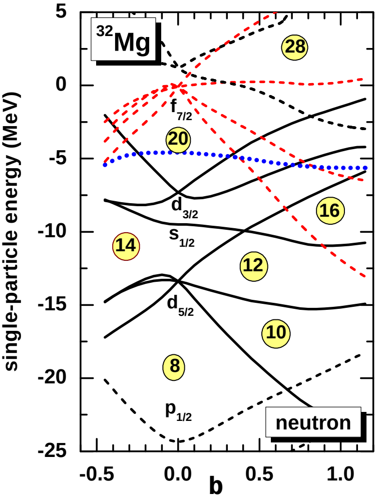

- Occupation of neutron *d*5/2 (or *f*7/2) orbits together with large shell gaps in the prolate side give rise to obvious minima in ^{22,24}Mg (or ^{36,38,40}Mg) respectively.

Nuclear shape and shell structure

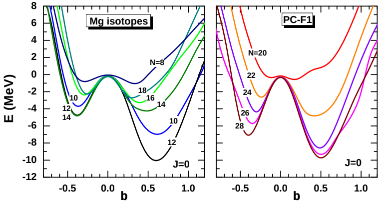

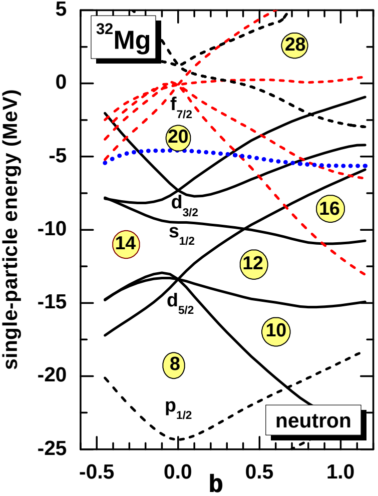

- Occupation of neutron $d5/2$ (or $f7/2$) orbits together with large shell gaps in the prolate side give rise to obvious minima in ^{22,24}Mg (or ^{36,38,40}Mg) respectively.
- Similar size of shell gaps in both prolate and oblate sides gives rise to two nearly-degenerate minima in ^{26,28,30}Mg.
- large (and small) spherical (prolate) $N = 20$ gap gives rise to the spherical ground state in ^{32}Mg.

E2 transition strengths

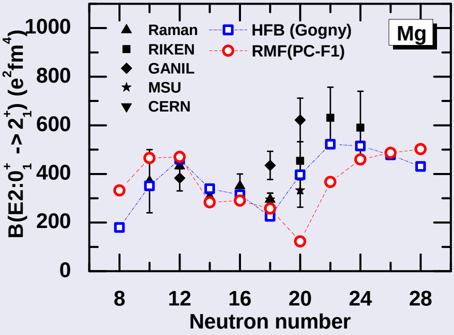

Figure: $B(E2; 0_1^+ \to 2_1^+)$ (e^2fm^4) values in $^{20-40}$Mg, calculated using the 1DAMP+GCM model with the relativistic density functional PC-F1, are compared to available data and the results of the 1DAMP+GCM calculation based on the non-relativistic HFB framework with the Gogny force *[Rodriguez-Guzman, Egido & Robledo, NPA709, 201 (2002)]*.

- By restricting axial symmetry, the calculations with PC-F1 yield results in reasonable agreement with data except at and in the neighborhood of the neutron number $N = 20$.
- The PC-F1 set gives spherical ground state for ^{32}Mg, which is contradict with the experimental result.
- Triaxality or pairing correlation?

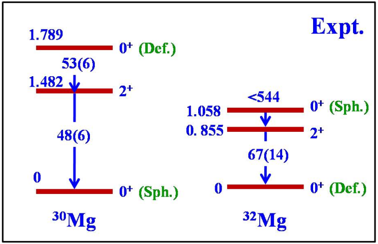

W. Schwerdtfeger et al., PRL 103, 012501 (2009)
K. Wimmer et al., PRL 105, 252501 (2010)

Potential energy surfaces in (β, γ) plane

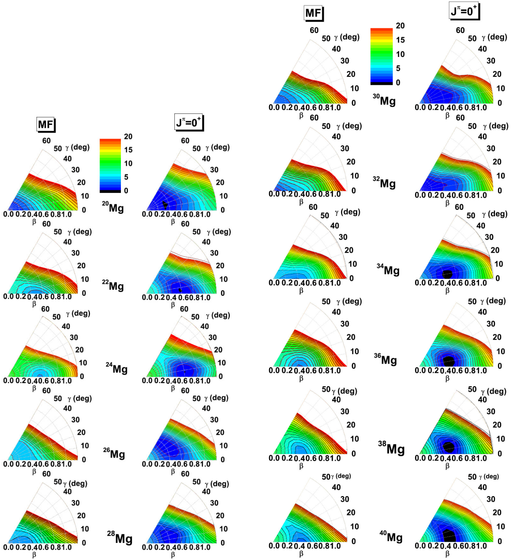

- Most of the oblate minima are actually saddle points in the (β, γ) plane.
- In ^{26,28,30}Mg, the PES is very soft through γ distortion.
- ^{32}Mg is β-soft in the neighborhood of spherical shape, indicating the strong mixing of spherical and prolate deformed shapes in ground state of ^{32}Mg.

Effect of triaxiality in magnesium isotopes

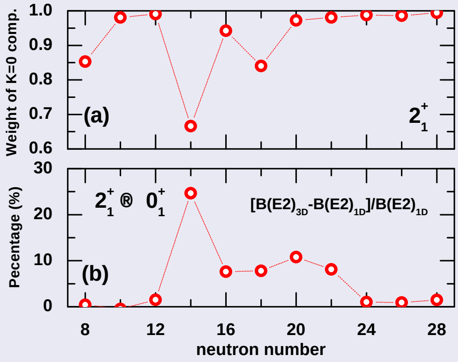

Figure: Upper panel: relative weight of the $K = 0$ component in the collective wave functions of the 2^+_1 states. Lower panel: differences between the $B(E2; 2^+_1 \to 0^+_1)$ values calculated in the 3DAMP+GCM and the 1DAMP+GCM models, normalized to the 1D values.

- Largest effect of triaxiality ($\sim 25\%$ enhancement) on $B(E2)$ value is found in ^{26}Mg.
- Moderate effect of triaxiality ($\sim 10\%$ enhancement) on $B(E2)$ value is found in $^{28-34}$Mg.

Effect of triaxiality in ^{30}Mg

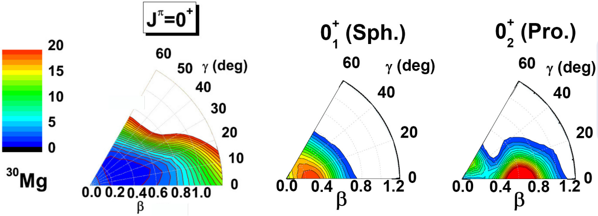

The projected PES ($J = 0$) and Probability distributions of $0^+_{1,2}$ states in β-γ plane.

Table: Results from 1D and 3DAMP+GCM calculations with the relativistic PC-F1 force and non-relativistic Gogny force, compared to experimental values. Both the non-relativistic calculation results and experimental data are taken from Ref.[*W. Schwerdtfeger et al., PRL 103, 012501 (2009)*].

	$E_x(2^+_1)$ (MeV)	$E_x(0^+_2)$ (MeV)	$\rho^2_{21}(E0)\times 10^3$	$B(E2;0^+_1\to 2^+_1)$ (e^2fm^4)	$B(E2;0^+_2\to 2^+_1)$ (e^2fm^4)
Exp.	1.482	1.789	26.2±7.5	241(31)	53(6)
3D(PC-F1)	1.721	2.864	24.72	277	68↑
1D(PC-F1)	1.882	3.275	15.56↓	257	47
1D(Gogny-D1S)	2.03	2.11	46 ↑	334.6	181.5↑

effect of pairing strengths in ^{30}Mg

effect of pairing strengths: 3D calculations

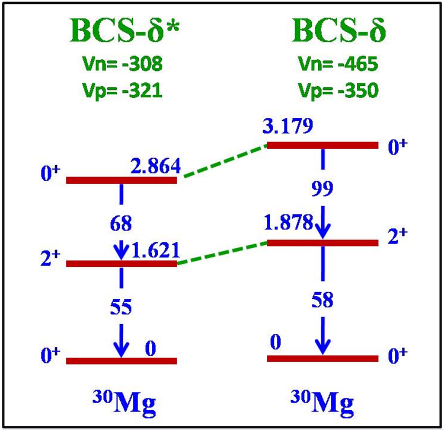

The pairing strengths are either chosen as the original ones (*BCS*-δ^*) in the PC-F1 set or determined by fitting to the experimental odd-even mass difference (*BCS*-δ).

- The increasing of pairing strengths reduces the MOI and therefore stretches the spectrum.

effect of pairing strengths in ^{32}Mg

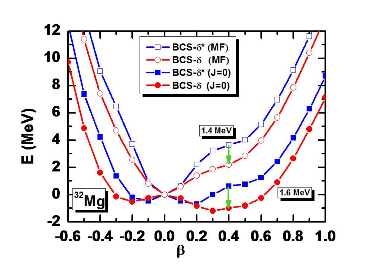

Adjustment of pairing strengths (fitted to odd-even mass diff.) can lower down the shoulder by 1.6 MeV. As a results, a prolate deformed minimum is shown on the projected ($J = 0$) PEC.

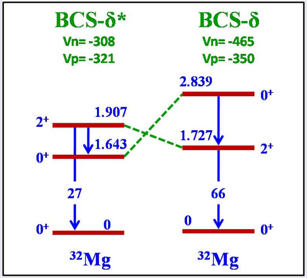

After considering the triaxiality, the $B(E2; 0_1^+ \to 2_1^+) = 330.1$ e^{2}fm^4 and the ordering of 2_1^+ and 0_2^+ states in ^{32}Mg are in good agreement with the data.

effect of pairing strengths in ^{32}Mg

Probability distributions:

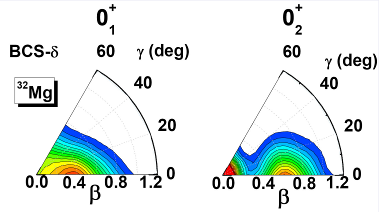

0_1^+: Prolate 0_2^+: Spherical and Prolate

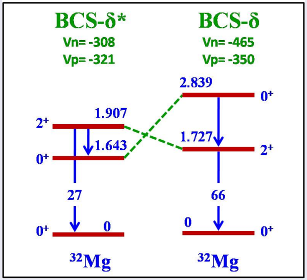

After considering the triaxiality, the $B(E2; 0_1^+ \rightarrow 2_1^+) = 330.1$ e^{2}fm^4 and the ordering of 2_1^+ and 0_2^+ states in ^{32}Mg are in good agreement with the data.

The increasing of pairing strengths breaks the $N = 20$ shell, as a consequence of which, the deformed $\nu(f_{7/2})^2(d_{3/2})^{-2}$ configuration becomes the ground state.

effect of triaxiality in ^{32}Mg

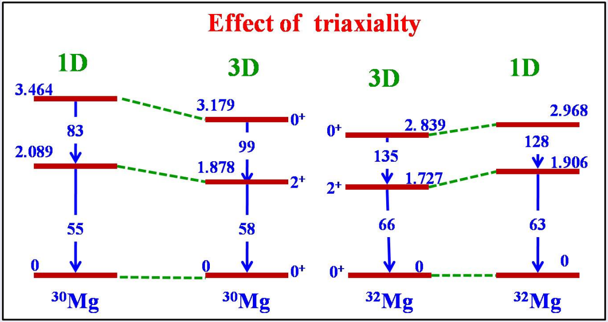

- Pairing strengths are adjusted by fitting to the experimental odd-even mass diff.
- The including of triaxiality reduces the excitation energy and enlarges the *E*2 transition strengths.

Outline

Summary

The relativistic version of 3DAMP+GCM approach and its applications

- The relativistic 3DAMP+GCM model has been developed and applied to study the low-lying states of magnesium isotopes. The spectroscopic properties of low-spin states, including excitation energy, $E0$, $E2$ transition strengthes, were studied. In particular, the effects of triaxiality and pairing correlation have been examined.
- Evident triaxial effects in $B(E2)$ value of ^{26}Mg and $E0$ transition of ^{30}Mg.
- Increasing of pairing correlation (to break the $N = 20$ shell) is essential to reproduce the data of ^{32}Mg.

Perspective

What is going on and what can be done in the near future?

- Using a separable pairing force in the pairing channel (close to be finished).
  In collaboration with Li, Niksic, Vretenar, Ring, & Meng
- Comparing with the same energy functional based Bohr Hamiltonian calculation to examine the Gaussian Overlap Approximation (in progress).
  In collaboration with Li, Niksic, Vretenar, Ring, & Meng
- Augmenting the particle number projection with regularization (scheduled)
  Lacroix, Duguet & Bender, PRC79, 044318 (2009).
  Bender, Duguet & Lacroix, PRC79, 044319 (2009).
- Extension for odd-A and odd-odd nuclei.
- . . .

Collaboration

Jie Meng	Peking Univ.
Peter Ring	TUM
Daniel Pena Arteaga	TUM
Dario Vretenar	Zagreb Univ.

Thanks for Your attention!

Potential energy curves as functions of β

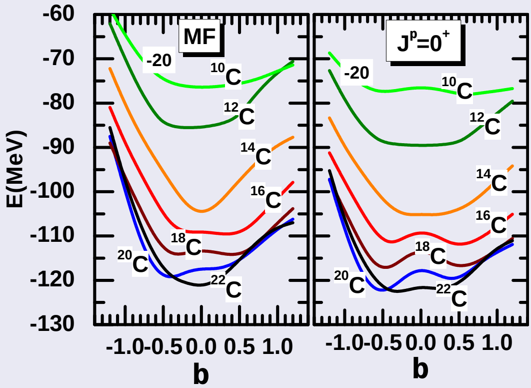

Figure: Self-consistent RMF+BCS mean-field and angular-momentum projected 0^+ potential energy curves of even-even carbon isotopes, as functions of the axial deformation parameter β.

Excitation energies and $B(E2)$ values in Carbon isotopes

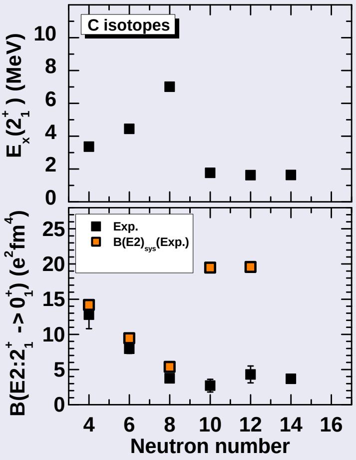

Figure: Excitation energies of 2_1^+ states $E_x(2_1^+)$ (MeV) and the $B(E2)$ values (e^2fm^4) for even-even carbon isotopes.

- The experiment $B(E2)$ values are compared with the prediction by the empirical relation: *S. Raman et al., PRC37, 805 (1988)*

$$B(E2: 0_1^+ \to 2_1^+)_{\rm sys.} = 6.47 Z^2 A^{-0.69} E_x^{-1}(2_1^+). \quad (6)$$

Excitation energies and $B(E2)$ values in Carbon isotopes

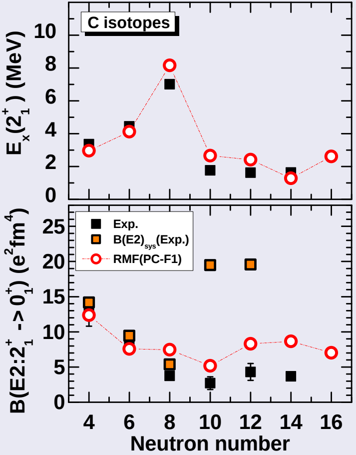

Figure: Excitation energies of 2_1^+ states $E_x(2_1^+)$ (MeV) and the $B(E2)$ values (e^2fm^4) for even-even carbon isotopes.

- The experiment $B(E2)$ values are compared with the prediction by the empirical relation: *S. Raman et al., PRC37, 805 (1988)*

$$B(E2:0_1^+ \to 2_1^+)_{\text{sys.}} = 6.47 Z^2 A^{-0.69} E_x^{-1}(2_1^+). \quad (6)$$

- The systematics of both $E_x(2_1^+)$ and $B(E2:2_1^+ \to 0_1^+)$ are reproduced quite well
- The quenched $B(E2)$ values, combined with the very low $E_x(2_1^+)$ indicate that the decoupled structure of neutron and proton exist in $^{16,18,20}C$.

Potential energy surfaces in (β, γ) plane

Potential energy surfaces:

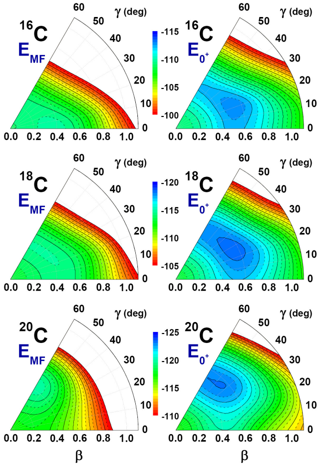

Probability distributions:

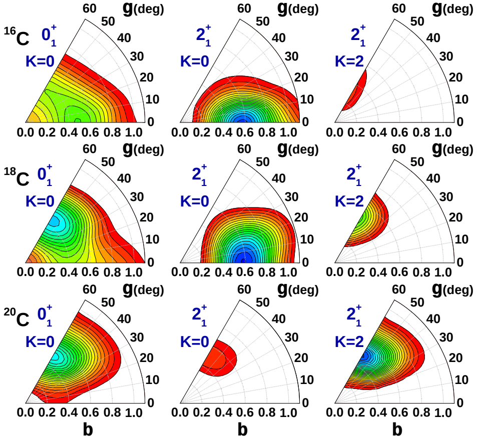

Potential energy surfaces in (β, γ) plane

Potential energy surfaces:

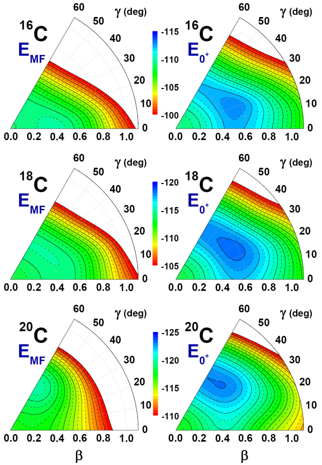

Single-particle energy levels of neutrons in ^{16}C:

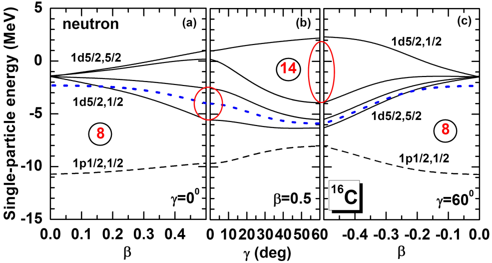

Effects of triaxiality in ^{16,18,20}C

Table: The excitation energies $E_x(J^\pi)$ (in MeV), and $B(E2\downarrow: J \to J-2)$ values (in e^2fm^4) for the lowest states with $J^\pi = 2^+, 4^+$ in ^{16,18,20}C. The average proton numbers $\langle Z \rangle$ of the calculated 2_1^+, 4_1^+ states are also given.

		Exp		3DAMP+GCM			1DAMP+GCM		
Nuclei	J^π	E_x	$B(E2\downarrow)$	E_x	$B(E2\downarrow)$	$\langle Z \rangle$	E_x	$B(E2\downarrow)$	$\langle Z \rangle$
^{16}C	2_1^+	1.766	$2.7 \pm 0.2 \pm 0.7$ [1] 4.15 (73) [2]	2.692	5.69	5.996	2.618	5.36	5.997
	4_1^+	4.142		7.068	10.66	5.999	6.877	10.60	5.997
^{18}C	2_1^+	1.585(10) [1]	$4.3 \pm 0.2 \pm 1.0$ [1]	2.162	8.55	5.994	2.477	8.57	5.995
	4_1^+			5.508	9.23	5.997	5.845	10.24	5.995
^{20}C	2_1^+	1.588(20) [3]	< 3.68 [3]	1.328	8.80	5.999	1.321	8.77	6.000
	4_1^+			4.824	13.46	5.999	4.822	13.39	6.000

[1] H. J. Ong *et al.*, Phys. Rev. **C78**, 014308 (2008).

[2] M. Wiedeking *et al.*, Phys. Rev. Lett. 100, 152501 (2008).

[3] Z. Elekes, Zs. Dombrádi, T. Aiba *et al.*, Phys. Rev. **C79**, 011302(R) (2009).

Potential energy surface of ^{14,22}C

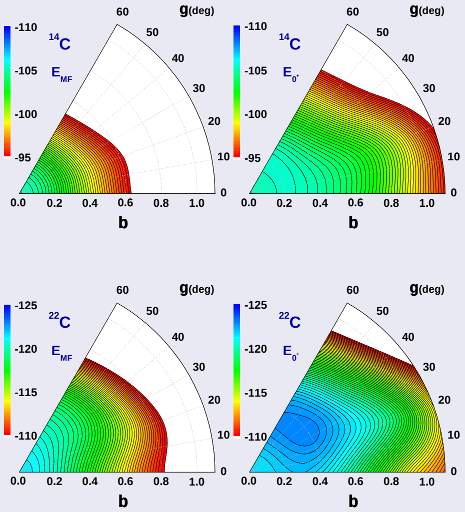

Probability distribution of low-lying states in ^{14,22}C